electronics

MDPI

Article

Galvanically Decoupled Current Source Modules for Multi-Channel Bioimpedance Measurement Systems

Roman Kusche *, Sebastian Hauschild and Martin Ryschka *

Laboratory of Medical Electronics (LME), Lübeck University of Applied Sciences, 23562 Lübeck, Germany; sebastian.hauschild@stud.fh-luebeck.de

* Correspondence: roman.kusche@fh-luebeck.de (R.K.); martin.ryschka@fh-luebeck.de (M.R.); Tel.: +49-451-300-5400 (R.K.)

Received: 25 August 2017; Accepted: 19 October 2017; Published: 23 October 2017

Abstract: Bioimpedance measurements have become a useful technique in the past several years in biomedical engineering. Especially, multi-channel measurements facilitate new imaging and patient monitoring techniques. While most instrumentation research has focused on signal acquisition and signal processing, this work proposes the design of an excitation current source module that can be easily implemented in existing or upcoming bioimpedance measurement systems. It is galvanically isolated to enable simultaneous multi-channel bioimpedance measurements with a very low channel-coupling. The system is based on a microcontroller in combination with a voltage-controlled current source circuit. It generates selectable sinusoidal excitation signals between 0.12 and 1.5 mA in a frequency range from 12 to 250 kHz, whereas the voltage compliance range is ±3.2 V. The coupling factor between two current sources, experimentally galvanically connected with each other, is measured to be less than −48 dB over the entire intended frequency range. Finally, suggestions for developments in the future are made.

Keywords: voltage-controlled current source; bioimpedance; multi-channel; multi-frequency; galvanic decoupling

1. Introduction

In the past several years, bioimpedance measurements have become more and more popular in biomedical engineering. This technique for determining the electrical behavior of living tissue can either be used to measure the impedance of interest once or its changes over time by transient measurements [1]. One exemplary application for single measurements is body composition scales [2–4]. Transient measurements can, for example, be executed for respiration monitoring or detection of muscle contractions [5,6]. Additionally, in some applications, such as the electrical impedance tomography (EIT) imaging technique [7,8], multi-channel measurement devices are required. One further application is the detection of the arterial pulse wave at different positions of the human body to obtain information about its velocity and changes in pulse morphology [1,9–11].

Since the complex electrical impedance of tissue depends on the frequency of the used excitation current, this effect can be used to obtain additional information [1].

There are several multi-channel bioimpedance measurement devices published in the literature [12–15]. Most of these publications focus either on the measurement setup itself or on the measurement of the voltage drop across the bioimpedance and the following signal processing. This leads to the assumption that excitation current sources are of course needed for bioimpedance measurements, but they are currently not the focus of ongoing research.

Therefore, the aim of this work is the development of system-independent multi-frequency current source modules for multi-channel applications that can be easily used in combination with existing measurement devices and systems developed in the future. Since there are many applications for

bioimpedance measurements, the requirements for each application are different. The used circuit topology of the implemented voltage-controlled current source in this work can therefore be an exemplary setup. Nevertheless, the principle of the presented galvanically decoupled modules can be used in combination with other implementations of the current source circuit. Applicable topologies are, for example, the "modified Howland current source" [16], the "enhanced Howland circuit" [17] or the "two op-amps-based current source" [18].

The exemplary configuration of the modules in this work is focused on two multi-channel bioimpedance measurement setups, which have similar requirements. The first intended application is the multi-channel impedance plethysmography for pulse wave analysis. To measure the velocity of the pulse wave within the arteries, at least two simultaneous bioimpedance measurements are necessary. Kaufmann et al. [9] have shown that the usage of measurement frequencies of up to 390 kHz do almost not affect the morphology of the detected pulse wave and lead to similar results. The second intended application is the electrical impedance myography for detecting muscle contractions. Especially for controlling prostheses or orthoses, the contractions of several muscles have to be detected simultaneously. A commonly used measurement frequency for this application is 50 kHz [19]. In both exemplary applications, that the measurement channels are positioned very close to each other and that a galvanic decoupling is indispensable have to be taken into account.

The introduced system is a microcontroller based current source, whose output current can be easily controlled by an external electronic system. The excitation current frequency can be chosen from seven discrete values in the range from 12 to 250 kHz, which allows the intended exemplary measurement applications. The source is able to generate constant root-mean-square (rms) values between 0.12 and 1.5 mA to facilitate compliance with the standard for medical electrical equipment (IEC60601-1). These currents can also be chosen from four pre-defined values. The pre-defined current and frequency values can be easily changed in the firmware according to the application's requirements.

To enable the usage of the system in combination with many various bioimpedance measurement systems, as many current source modules as necessary can be connected and controlled in daisy chain mode.

This work describes the problem of simultaneous multi-channel bioimpedance measurements and the development of the embedded decoupled current source modules as well as its electrical characterization.

2. Problem Description

Bioimpedance measurements are usually executed by applying a small known alternating current (AC) in the mA-range through electrodes attached on the skin into the tissue of interest. Since the electrode skin interface (ESI) impedances are much higher than the bioimpedance itself and vary significantly over time [1,19], two additional electrodes are used to measure the occurring voltage drop across the bioimpedance [1]. This differential voltage is fed to a differential amplifier.

If two or more measurement channels shall be implemented to determine the bioimpedance at different positions of the body at the same time, obviously several current sources and differential amplifiers are connected to the subject via electrodes. The resulting problem of this measurement configuration is shown in the simplified equivalent circuit in Figure 1a. In this simplification, it is assumed that the internal resistances of the two current sources (CS1, CS2) as well as the input impedances of the differential amplifiers are much higher than the bioimpedances (Z_{Bio}) and the electrode skin interface impedances (Z_{ESI}). Therefore, the current sources and amplifiers are simplified as ideal components. In the equivalent circuit, it can be seen that the excitation current I_2 of source CS2 is divided into two parts (I_{2a} and I_{2b}). Since the GND electrodes of both channels are connected to the same electrical potential, I_{2a} flows back to the correct electrode, but I_{2b} does not. This behavior influences the voltage drop across the bioimpedance of interest (Z_{Bio2}) and consequently the measurement results. Since the quantitative impact of this effect is not predictable and changes over time, it has to be prevented.

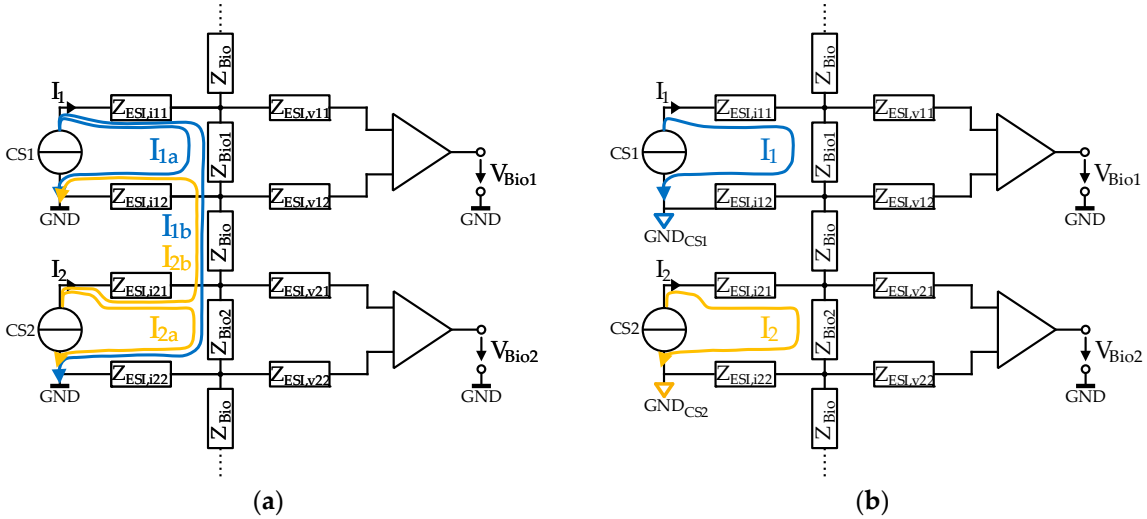

Figure 1. Simplified equivalent circuit of a simultaneous 2-channel bioimpedance measurement without (**a**) and with (**b**) galvanic decoupling of the current sources.

An often implemented solution for this problem is the compartmentation in time domain by multiplexing the excitation currents [1,7]. A major advantage of this realization is that just one current source circuit is necessary. Disadvantages are the complex control of the multiplexers and the subsequent synchronization of the measured voltage signals. Additionally, the settling processes of the analog circuit components have to be considered. These settling processes limit the impedance measurement rate especially when low excitation frequencies are used.

Another approach, which also enables simultaneous measurements, is the galvanic isolation of the current sources, as shown in Figure 1b. In this figure, both current source circuits are realized with different GND potentials (GND_{CS1}, GND_{CS2}), which are galvanically isolated. Therefore, each current flows back to its intended electrode. Furthermore, the data interfaces, which control the configuration of the current source modules, have to be isolated, too. Because of its very high input impedances, the differential amplifiers can be fed by the same power supply. This work describes the implementation of this approach.

3. System Development

For highest flexibility, an embedded hardware system has been developed, which can easily be combined with existing bioimpedance measurement systems. In Figure 2, a block diagram of the designed system is shown.

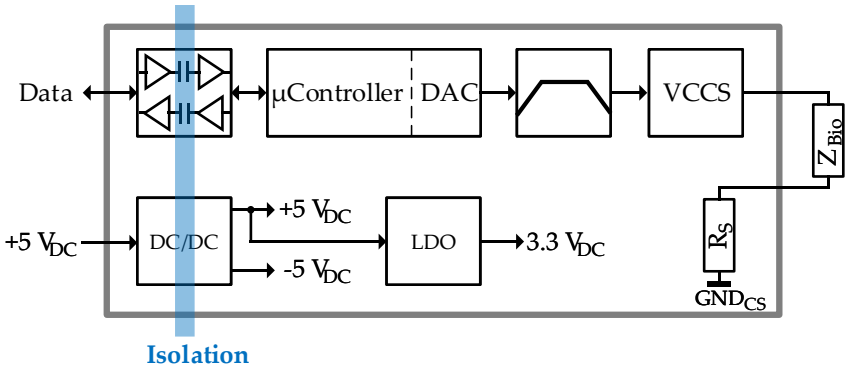

Figure 2. Block diagram of the developed decoupled current source module.

The current source module is powered by 5 V_{DC} from an external voltage supply or by a controlling bioimpedance measurement system. An isolating DC/DC converter (MTU2D0505MC (Murata Power Solutions, Nagaokakyō, Japan)) is used to implement the galvanic separation of the power supply and to generate a bipolar voltage supply of ±5 V_{DC}, which is used for the analog components of the system. The output voltages of the DC/DC converter are filtered by passive LC-filters with a cut-off frequency of 23 kHz, as suggested in the data sheet. To generate 3.3 V_{DC} for the digital components, a low dropout regulator (LDO, TPS73033 (Texas Instruments, Dallas, TX, USA)) is used.

The data exchange between a controlling measurement system and the current source module is also galvanically isolated. For this purpose, digital isolators (ISO7220BD, ISO7221BD from Texas Instruments), which allow signal rates of up to 5 Mbps, are implemented. The thereby received configuration data is forwarded to a 32-bit microcontroller (ATSAM4S2BA (Atmel Corporation, San José, CA, USA)), which generates a digital sinusoidal signal with the chosen frequency (12–250 kHz) and root-mean-square (rms) current value (0.12–1.5 mA). Its internal 12-bit digital to analog converter (DAC), with a sampling rate of 1 MSPS, generates the corresponding AC voltage. An active 4th order Butterworth low-pass filter in multiple-feedback topology with a cut-off frequency of f_c = 400 kHz is realized by two operational amplifiers (LMH6646 from Texas Instruments) to smooth the sampled signal. Afterwards, the remaining DC offset voltage is removed by a passive 1st-order high-pass filter with a cut-off frequency of f_c = 200 Hz. A voltage-controlled current source (VCCS), which is based on the AD8130 (Analog Devices Inc., Norwood, MA, USA) [9,20], converts the voltage signal into an AC current. This current flows via the electrodes through the bioimpedance (Z_{Bio}) and a shunt resistor (R_S = 69.8 Ω).

In Figure 3, the circuit diagram of the analog filter block is illustrated. The implemented resistors have tolerances of 1%. To avoid signal harmonics caused by non-linarities, class 1 ceramic capacitors with tolerances of 5% are used. The filtered signal is afterwards buffered by an OPA2134 (from Texas Instruments).

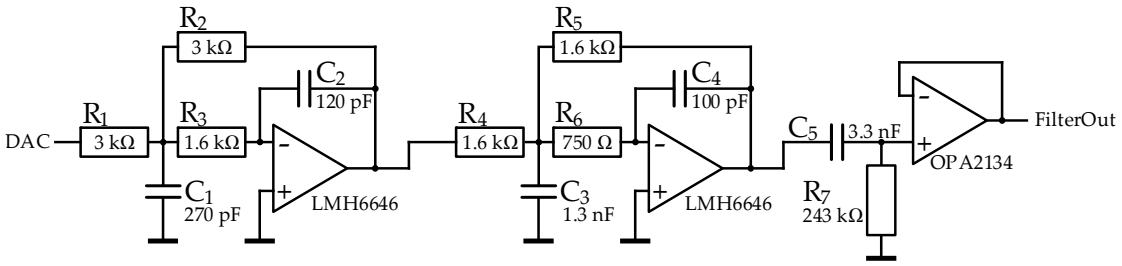

Figure 3. Circuit diagram of the analog low pass and high pass filter.

The circuit diagram of the subsequent voltage-controlled current source, based on the published circuits of Zhao et al. [20] and Kaufmann et al. [9], is shown in Figure 4. Its transfer function is given in Equation (1).

$$\frac{I_{out}}{V_{in}} = -\frac{1}{R_9} = -2.7\frac{mA}{V}. \quad (1)$$

The components' tolerances as well as the class 1 characteristic of the capacitors are the same as described for the filter block before.

The modules are realized on 4-layer printed circuit boards (PCBs) with a size of 23 × 126 mm^2 and have a weight of 23 g, when the 102 components are populated. A photograph of three modules connected in daisy chain mode is shown in Figure 5.

Each PCB has a power consumption of about 620 mW when active and generating a current of 1.5 mA, whereas the output frequency does not have a significant impact on this consumption.

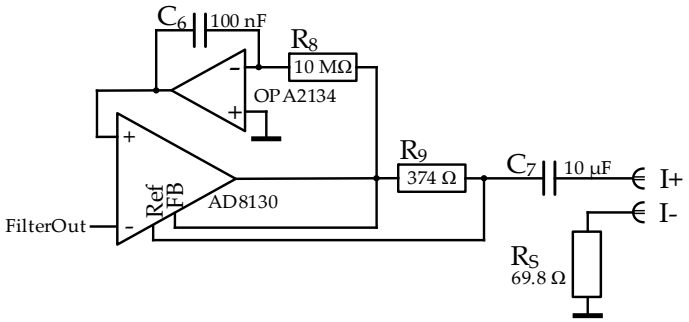

Figure 4. Circuit diagram of the implemented voltage-controlled current source.

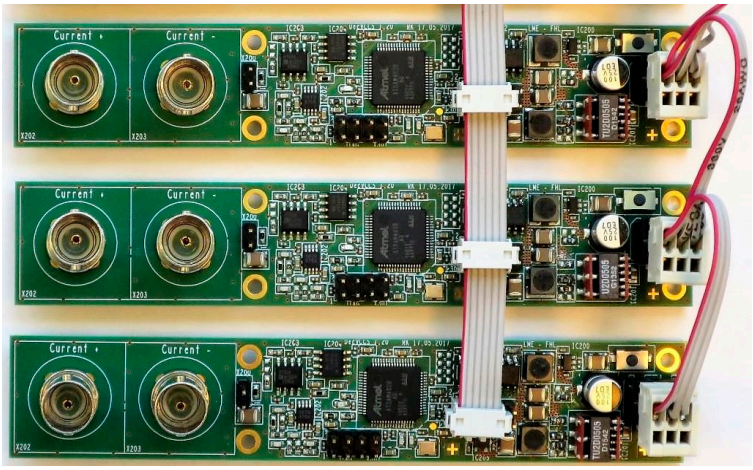

Figure 5. Photograph of three current source modules, connected in daisy chain mode.

Table 1 shows the format of the data frame for configuring the current source modules. It can be seen that Bit 7, Bit 6, and Bit 5 contain the information about the chosen frequency. Bit 4 can be used to enable or disable the source. Bit 3 and Bit 2 configure the signal's rms value. The address of the corresponding module is set in Bit 1 and Bit 0. These two address bits lead to a limitation of four modules connected in daisy chain mode, but it can be easily extended by minor software adaptions.

Table 1. Data frame for current source configuration.

Bit 7	Bit 6	Bit 5	Bit 4	Bit 3	Bit 2	Bit 1	Bit 0
Frequency	Frequency	Frequency	Activation	rms Value	rms Value	Address	Address

Previously to these 8 bits, a transmission start bit has to be sent by the controlling device. By measuring its duration, the microcontroller can calculate the expected data transmission rate of the controller. This leads to the advantage that any transmission rate can be used without firmware changes. It is just limited by the digital isolators to a maximum rate of 5 Mbps.

4. Results

In this section, the performance of the developed current source modules is characterized. The signal-to-noise and distortion (SINAD) ratio as well as the load characteristic are determined. Finally, the efficiency of decoupling is analyzed.

4.1. Quality of Generated Sinusoidal Signals

Since bioimpedances are frequency-dependent [1], it is important to ensure that the excitation frequency is generated reliably and that distortions are minimized. To determine the signal quality of the current source, a 1 kΩ load resistor is connected as known load impedance to a module using cables with a length of 1 m. An output current of 1.5 mA is applied to this load and the occurring voltage drop over the resistor is measured by a 12-bit digital oscilloscope (HDO6054 (Teledyne LeCroy, Chestnut Ridge, NY, USA)) for a duration of 50 ms. The measurement is repeated for all 7 selectable frequencies (12 kHz, 30 kHz, 50 kHz, 77 kHz, 143 kHz, 200 kHz, 250 kHz). In Figure 6, the resulting normalized magnitude spectrum of a 30 kHz current is exemplary shown. It can be seen that the harmonics are attenuated by at least 60 dB.

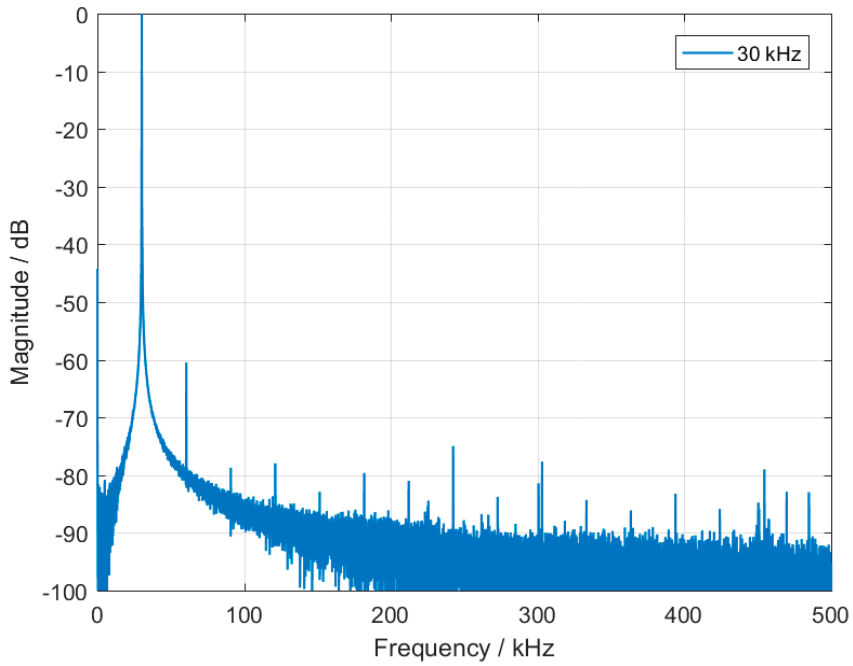

Figure 6. Normalized magnitude spectrum of a 1.5 mA output current signal with a frequency of 30 kHz, measured over a 1 kΩ resistor.

In Table 2, the resulting SINAD values are shown for each frequency. The signal quality of low frequency signals is better than these of high frequency signals. The reason for this effect is that the image frequency at f_s-f_{signal} comes closer to the cut-off frequency of the low-pass filter after the DAC.

Table 2. Signal-to-noise and distortion (SINAD) ratio of the generated 1.5 mA current signal over frequency, measured over a 1 kΩ resistor.

Frequency/kHz	**12**	**30**	**50**	**77**	**143**	**200**	**250**
SINAD/dB	46.3	46.3	46.0	44.9	40.6	35.0	32.1

4.2. Load Characteristic of the Current Source

Even when the actual current, injected into the bioimpedance, can be determined by measuring the voltage drop over the shunt resistor, it is desirable to generate reliable currents that do not change over load impedance. To determine the influence of the load resistance on the output current, the current source is connected to 30 different load resistances in a range from 31.6 Ω to 1 MΩ. This measurement is repeated for three excitation frequencies (30 kHz, 77 kHz, and 200 kHz) with a constant output

current of 1.5 mA to check if there is an additional frequency dependency. The occurring voltage drop over the load is measured by a 12-bit digital oscilloscope (HDO6054 from Teledyne LeCroy).

In Figure 7, the actual output current (I_{rms}) is plotted over load resistance (R_L) for these three frequencies. Up to a load resistance of about 1500 Ω the output current for each frequency is very stable, which represents a maximum compliance voltage range of ±3.2 V. The current changes over the entire range less than 2%. The attenuation in the 200 kHz plot of about 0.1 mA, which is constant over the load, is caused by the low-pass filter characteristic and does not have a negative influence on impedance measurements. It can easily be calibrated.

The resulting output impedances, calculated with the data points at R_L = 10 Ω and R_L = 1.21 kΩ, are $|Z_{out,\ 30\ kHz}|$ = 89 kΩ, $|Z_{out,\ 77\ kHz}|$ = 68 kΩ, and $|Z_{out,\ 200\ kHz}|$ = 49 kΩ.

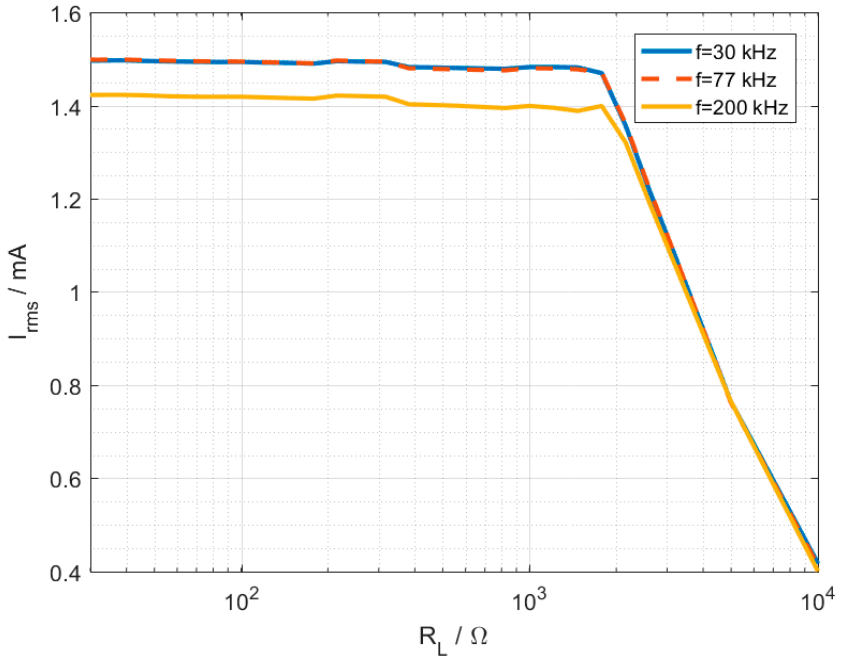

Figure 7. Output current of the current source depending on the load resistance and signal frequency. The output current was 1.5 mA.

It can be assumed that this behavior does not change significantly when generating lower current amplitudes.

4.3. Efficiency of Decoupling

To measure the efficiency of the galvanic decoupling, two current source modules are connected to load resistances of R_{L1} = R_{L2} = 1 kΩ each, as shown in Figure 8. Additionally, the outputs are connected with each other to model a simple ideal coupling. Both modules are powered by the same external voltage source and are just isolated by the DC/DC converters as described before.

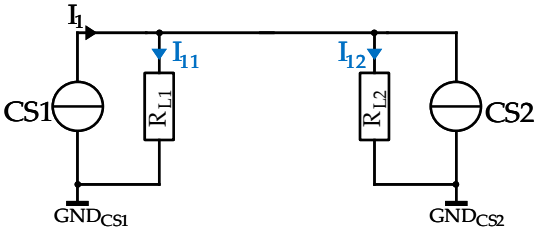

Figure 8. Measurement setup to determine the coupling between the current sources CS1 and CS2.

CS1 generates an output current of 1.5 mA, whereas the output of CS2 is switched off. The coupling factor (CF) between both the sources is then determined by measuring I_{11} and I_{12} and the usage of Equation (2).

$$\mathrm{CF} = 20 \times \log_{10}\left(\frac{I_{12}}{I_{11}}\right)\mathrm{dB}. \tag{2}$$

The resulting coupling factors are plotted in Figure 9 over frequency. As expected, the decoupling decreases with higher frequencies due to the parasitic capacity of the DC/DC converter. Nevertheless, the coupling between both modules is less than −48 dB over the entire frequency range. That the decoupling does not work as well as expected when generating a 12 kHz signal can be explained by the cut-off frequency of the LC low-pass filter at the output of the DC/DC converter, which is 23 kHz, as described before.

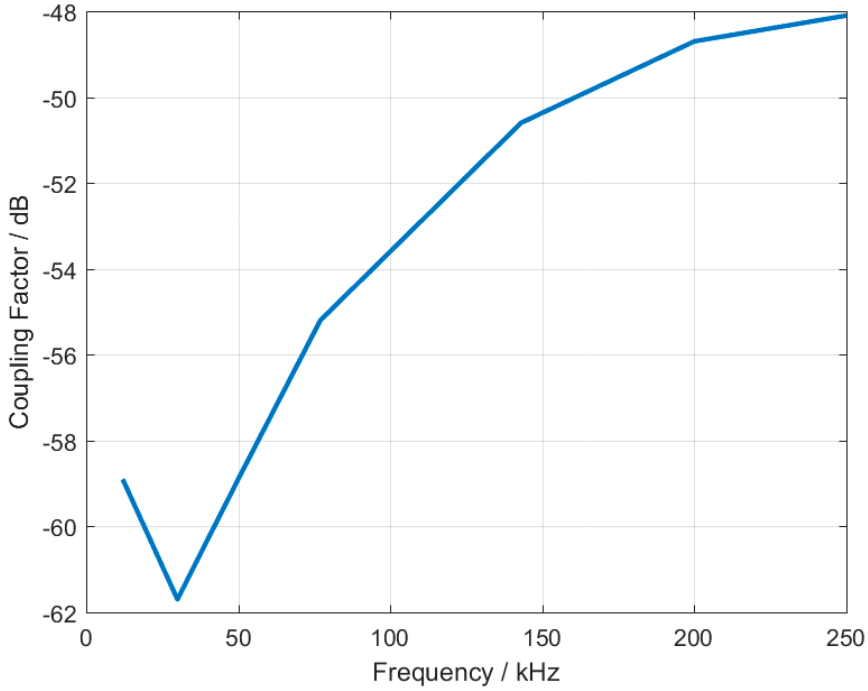

Figure 9. Coupling between the current sources over frequency.

In real bioimpedance measurement environments, the actual coupling between channels is of course even lower than these values but impossible to predict. Since the simplified network in Figure 6 as well as the more complex network in Figure 1 are assumed to be linear, further measurements with complex impedances or with different frequencies are not necessary.

5. Summary and Outlook

We have here described the problem of multi-channel bioimpedance measurements and discussed the difference between solving this issue by multiplexing and by galvanic isolation of the current sources. Afterwards, we explained the development of galvanically isolated current source modules, with a focus on the electrical circuitry. These modules are capable of generating excitation currents of up to 1.5 mA in a frequency range from 12 to 250 kHz and can be easily controlled by existing bioimpedance measurement systems. The selectable current values as well as the frequency values are pre-defined in the firmware for exemplary applications of multi-channel electrical impedance plethysmography and myography, but can easily be changed or extended for a specific application if necessary.

After the determination of the current signal quality, the load characteristic of the source was analyzed. The current stability is higher than 98% when used within the compliance range of ±3.2 V. To measure the coupling factor between two current sources, whose current outputs are connected with each other, a simple measurement setup was presented. The resulting measured coupling factors were for the entire frequency range of the current source modules lower than 48 dB.

In the future, the size, weight, and power consumption of these modules should be reduced, to enable usage within wearable systems. Depending on the application and on the used measurement system, which controls the modules, changes in the communication protocol are advisable. It is conceivable that some applications need, for example, more or different signal frequencies than in this work suggested. Additionally, the implementation of multi-frequency excitation currents, such as chirp signals [21], might be useful in the future. Some measurement applications might also need a different current source circuit topology.

Furthermore, existing but currently unused general purpose inputs/outputs (GPIOs) of the modules could be used for synchronization purposes.

Acknowledgments: This work has been supported by the German Federal Ministry of Education and Research (BMBF) under the project INOPRO (FKZ16SV7666).

Author Contributions: R.K. designed the hardware as well as the software of the current version of the described system. R.K. also wrote this paper. S.H. developed the initial version of the system's hard- and software and developed the galvanically isolated power supply. M.R. supervised the entire research project and the writing of this paper.

Conflicts of Interest: The authors declare no conflict of interest.

References

1. Grimnes, S.; Martinsen, O.G. *Bioelectricity and Bioimpedance Basics*, 2nd ed.; Academic Press: Cambridge, MA, USA, 2008.
2. Lee, S.Y.; Gallagher, D. Assessment methods in human body composition. *Curr. Opin. Clin. Nutr. Metab. Care* **2008**, *11*. [CrossRef] [PubMed]
3. Matthie, J.R. Bioimpedance measurements of human body composition: Critical analysis and outlook. *Expert Rev. Med. Devices* **2008**, *5*. [CrossRef] [PubMed]
4. Grimnes, S.; Martinsen, O.G. Bioimpedance. In *Wiley Encyclopedia of Biomedical Engineering*; John Wiley and Sons, Inc.: New York, NY, USA, 2006; pp. 438–447.
5. Koivumäki, T.; Vauhkonen, M.; Kuikka, J.T.; Hakulinen, M.A. Bioimpedance-based measurement method for simultaneous acquisition of respiratory and cardiac gating signals. *Physiol. Meas.* **2012**, *33*. [CrossRef] [PubMed]
6. Rutkove, S.B. Electrical impedance myography: Background, current state, and future directions. *Muscle Nerve* **2009**, *40*. [CrossRef] [PubMed]
7. Kusche, R.; Malhotra, A.; Ryschka, M.; Ardelt, G.; Klimach, P.; Kaufmann, S. A FPGA-Based Broadband EIT System for Complex Bioimpedance Measurements—Design and Performance Estimation. *Electronics* **2015**, *4*. [CrossRef]
8. Cherepenin, V.; Karpov, A.; Korjenevsky, A.; Kornienko, V.; Mazaletskaya, A.; Mazourov, D.; Meister, D. A 3D electrical impedance tomography (EIT) system for breast cancer detection. *Physiol. Meas.* **2001**, *22*, 9–18. [CrossRef] [PubMed]
9. Kaufmann, S.; Malhotra, A.; Ardelt, G.; Ryschka, M. A high accuracy broadband measurement system for time resolved complex bioimpedance measurements. *Physiol. Meas.* **2014**, *35*, 6. [CrossRef] [PubMed]
10. Luna-Lozano, P.S.; Pallàs-Areny, R. Heart rate detection from impedance plethysmography based on concealed capacitive electrodes. In Proceedings of the XIX IMEKO World Congress, Lisbon, Portugal, 6–11 September 2009.
11. Kusche, R.; Adornetto, T.D.; Klimach, P.; Ryschka, M. A Bioimpedance Measurement System for Pulse Wave Analysis. In Proceedings of the 8th International Workshop on Impedance Spectroscopy, Chemnitz, Germany, 23–25 September 2015.

12. Oh, T.I.; Wi, H.; Kim, D.Y.; Yoo, P.J.; Woo, E.J. A fully parallel multi-frequency EIT system with flexible electrode configuration: KHU Mark2. *Physiol Meas.* **2011**, *32*. [CrossRef] [PubMed]
13. Stanley, A.W.; Herald, J.W.; Athanasuleas, C.L.; Jacob, S.C.; Bartolucci, A.A.; Tsoglin, A.N. Multi-channel electrical bioimpedance: A non-invasive method to simultaneously measure cardiac output and individual arterial limb flow in patients with cardiovascular disease. *J. Clin. Monit. Comput.* **2009**, *23*. [CrossRef] [PubMed]
14. Halter, R.J.; Hartov, A.; Paulsen, K.D. A broadband high-frequency electrical impedance tomography system for breast imaging. *Trans. Biomed. Eng.* **2008**, *55*. [CrossRef] [PubMed]
15. Avery, J.; Dowrick, T.; Faulkner, M.; Goren, N.; Holder, D. A Versatile and Reproducible Multi-Frequency Electrical Impedance Tomography System. *Sensors* **2017**, *17*. [CrossRef] [PubMed]
16. Bera, T.K.; Jampana, N. A multifrequency constant current source suitable for Electrical Impedance Tomography (EIT). In Proceedings of the International Conference on Systems in Medicine and Biology (ICSMB), Kharagpur, India, 16–18 December 2010.
17. Ross, A.S.; Saulnier, G.J.; Newell, J.C.; Isaacson, D. Current source design for electrical impedance tomography. *Physiol. Meas.* **2003**, *24*, 509–516. [CrossRef] [PubMed]
18. Tietze, U.; Schenk, C. *Electronic Circuits: Handbook for Design and Application*; Springer: Berlin/Heidelberg, Germany, 2008.
19. Kaufmann, S.; Ardelt, G.; Ryschka, M. Measurements of Electrode Skin Impedances using Carbon Rubber Electrodes—First Results. In Proceedings of the XV International Conference on Electrical Bio-Impedance (ICEBI) & XIV Conference on Electrical Impedance Tomography (EIT), Heilbad Heiligenstadt, Germany, 22–25 April 2013.
20. Zhao, X; Kaufmann, S.; Ryschka, M. A comparison of different multi-frequency Current Sources for Impedance Spectroscopy. In Proceedings of the 5th International Workshop on Impedance Spectroscopy, Chemnitz, Germany, 26–28 September 2012.
21. Paavle, T.; Min, M.; Parve, T. Aspects of using chirp excitation for estimation of bioimpedance spectrum. In *Fourier Transform—Signal Processing*; Salih, S.M., Ed.; InTech: Rijeka, Croatia, 2012; pp. 237–256.